

NASA
TP
1751
c.1

NASA Technical Paper 1751

LOAN COPY: R
AFWL TECHNICAL
KIRTLAND AFB

0067668



TECH LIBRARY KAFB, NM

A New Look at Numerical Analyses of Free-Edge Stresses in Composite Laminates

I. S. Raju, J. D. Whitcomb, and J. G. Goree

DECEMBER 1980

NASA



NASA Technical Paper 1751

A New Look at Numerical Analyses of Free-Edge Stresses in Composite Laminates

I. S. Raju

The George Washington University

Joint Institute for Advancement of Flight Sciences

Langley Research Center

Hampton, Virginia

J. D. Whitcomb

Langley Research Center

Hampton, Virginia

J. G. Goree

Clemson University

Clemson, South Carolina

NASA

National Aeronautics
and Space Administration

**Scientific and Technical
Information Branch**

1980



SUMMARY

The edge-stress problem for a $[\pm 45]_S$ graphite/epoxy laminate was examined in detail. A review of the literature on this problem showed that the interlaminar normal stress σ_z distributions along the interface between the $+45^\circ$ and -45° plies, obtained by various investigators, disagreed in magnitude and sign. In particular, a finite difference solution and a perturbation solution predicted a tensile σ_z , whereas the finite element methods predicted a compressive stress. Since a stress singularity exists at the intersection of the interface and the free edge, the differences in magnitude of the peak stress were expected, but not the difference in the sign.

This paper investigates the reliability of the displacement-formulated finite element method in analyzing the edge-stress problem. Analyses of two well-known elasticity problems, one involving a stress discontinuity and one a singularity, showed that the finite element analysis yields accurate stress distributions everywhere except in two elements closest to the stress discontinuity or singularity. Stress distributions for a $[\pm 45]_S$ laminate showed the same behavior near the singularity as found in the well-known problems with exact solutions. The displacement-formulated finite element method, therefore, appears to be a highly accurate technique for calculating interlaminar stresses in composite laminates. The disagreement among the numerical methods was attributed to the unsymmetric stress tensor at the singularity.

INTRODUCTION

Delamination is a critical failure mechanism for laminated composite materials. Before delamination can be predicted, analyses must be developed to accurately calculate the interlaminar stresses that cause delamination. Several attempts have been made to obtain accurate stress distributions in a finite-width laminate subjected to uniform axial strain (refs. 1 to 10). Finite difference (refs. 1 and 3), boundary-layer theory (ref. 4), extended Galerkin method (ref. 7), and finite element method (refs. 2, 6, 8, 9, and 10) were used in these studies.

For the angle-ply laminate, $[\pm 45]_S$, the interlaminar normal stress distributions obtained by various investigators disagree in both magnitude and sign. Since a stress singularity exists at the intersection of the free edge and the interface (ref. 10), the differences in magnitude were expected but the differences in the sign were not.

A possible source of these discrepancies is the way different numerical methods behave near stress singularities. Verification of a particular analysis is complicated by the lack of an exact solution for the edge-stress problem. However, if an analysis can be shown to behave correctly for similar problems that do have exact solutions, one's confidence in the analysis is bolstered.

In this vein, the present paper investigates the use of displacement formulated finite element analysis for solving the edge-stress problem. First, the history of the edge-stress problem is reviewed. Next, the reliability of the finite element method for computing edge stresses is investigated. Finally, discrepancies between the finite element solution and other numerical solutions for the edge-stress problem are discussed.

SYMBOLS

b	semiwidth of the straight-edge laminate, m
E	Young's modulus for isotropic material, MPa
E_{ii}	Young's modulus for orthotropic material in the i -direction, MPa
G_{ij}	shear modulus for orthotropic material, MPa
h	ply thickness, m
p	pressure, kPa
U, V, W	displacement functions, m
u, v, w	displacements in the x -, y -, and z -directions, m
x, y, z	Cartesian coordinates, m
ϵ_0	uniform axial strain in the x -direction ($\epsilon_0 = 0.001$)
θ	angle between x axis and longitudinal axis (see fig. 1(a)), deg
ν	Poisson's ratios for isotropic material
ν_{ij}	Poisson's ratios for orthotropic material
$\{\sigma\}$	Cartesian stresses (see fig. 1(c)), MPa

Subscripts:

i	1, 2, 3
j	1, 2, 3
1, 2, 3	longitudinal, transverse, and thickness directions, respectively, of a unidirectional ply

DESCRIPTION OF THE EDGE-STRESS PROBLEM

Figure 1(a) shows a long, symmetric laminate loaded in the x -direction. The laminate has a width of $2b$ and has four plies, each of thickness h . Away

from the ends the displacement in any $x = \text{Constant}$ plane (fig. 1(b)) were assumed to be

$$\left. \begin{aligned} u(x,y,z) &= \epsilon_0 x + U(y,z) \\ v(x,y,z) &= V(y,z) \\ w(x,y,z) &= W(y,z) \end{aligned} \right\} \quad (1)$$

where ϵ_0 is a uniform axial strain, and U, V, W are functions of coordinates y and z alone. (See ref. 1.)

In the analyses each ply is idealized as a homogeneous, elastic orthotropic material with the following properties (refs. 1 to 10):

$$\begin{aligned} E_{11} &= 137.9 \text{ GPa} && (20 \times 10^6 \text{ psi}) \\ E_{22} = E_{33} &= 14.48 \text{ GPa} && (2.1 \times 10^6 \text{ psi}) \\ G_{12} = G_{23} = G_{13} &= 5.86 \text{ GPa} && (0.85 \times 10^6 \text{ psi}) \\ \nu_{12} = \nu_{23} = \nu_{13} &= 0.21 \end{aligned}$$

The subscripts 1, 2, and 3 correspond to the longitudinal, transverse, and thickness directions, respectively, of a unidirectional ply.

For convenience, the intersection of the interface between plies and the face edge ($z = h$; $y = b$ in fig. 1(b)) will be referred to as the interface corner. Also, the applied uniform axial strain ϵ_0 was arbitrarily set equal to 0.001 throughout the study.

SURVEY OF THE LITERATURE

The edge-stress problem for composite materials has received considerable attention in recent literature. However, significant disagreement still exists in the computed stress distributions for specific laminates. Table I summarizes the work of some particular investigators.

For $[0/90]_s$ and $[90/0]_s$ laminates, the stress distributions obtained by most investigators agree qualitatively. However, for $[+45]_s$ laminates considerable disagreement exists. As previously mentioned, the interlaminar normal stress σ_z very near the interface corner, obtained by various investigators, was found to differ in both magnitude and sign depending on the particular numerical technique used and the manner in which the free-edge condition was accounted for. Figure 2 illustrates the disagreement by comparing σ_z distributions along the interface (refs. 1, 5, 6, and 10). At the interface corner, Pipes and Pagano (ref. 1) and Hsu and Herakovich (ref. 5) obtained a tensile

value of σ_z . However, Hsu and Herakovich (ref. 5) also reported a compressive value of σ_z obtained with a finite difference program of Pipes (ref. 3). They attributed the negative value to the numerical instability in the finite difference solution. Finite element solutions by Wang and Crossman (ref. 6) and Raju and Crews (ref. 10) also gave compressive values of σ_z . (The σ_z stress was plotted with an incorrect sign in ref. 6, as confirmed by a personal communication with Wang. All the results of the finite element solutions of Wang and Crossman presented in this paper were obtained independently by the present authors with the same element and idealization as in ref. 6. These independent computations were made to facilitate comparisons of stress distributions which were not reported in ref. 6.) Tang and Levy (ref. 4) obtained a zero value for σ_z . Herakovich et al (ref. 8) did not present σ_z distributions along the interface.

Because of steep stress gradients near the free edge, all investigators except those in reference 9 speculated that a stress singularity exists at the interface corner. In fact, Raju and Crews (ref. 10) showed that stress singularities exist for $[\theta/(\theta-90)]_S$ laminates, where $0 \leq \theta \leq 90$.

It is well known that singular points present difficulties in numerical and approximate methods and that different numerical methods certainly behave differently near such singular points. Further, the behavior of a numerical solution near a singularity depends on how well the continuum is modeled and what numerical techniques are used near the singular points. All of these factors possibly contribute to the discrepancies in figure 2.

The finite element methods in references 6, 8, and 10 are displacement formulations based on the total potential energy theorem. They did not explicitly account for a stress singularity. Therefore, they did not model exactly the stresses at the singular point. It is important to investigate whether a finite element solution behaves in a consistent and reliable manner near singularities and whether accurate stress distributions can be obtained arbitrarily close to the singularity by progressive mesh refinement. The present paper addresses these questions.

First, for illustration, some observations are noted regarding the behavior of stresses near a stress discontinuity or a stress singularity. Second, finite element solutions are examined for two well-known problems involving stress discontinuities and singularities. Lastly, with the insight gained from these problems the finite element solutions for the edge-stress problem are studied. The differences between the present finite element solution and other numerical methods are discussed.

STRESSES AT DISCONTINUITIES AND SINGULARITIES

Both stress discontinuities and singularities have unbounded first partial derivatives of stress components. For numerical methods, this leads to obvious modeling difficulties in the localized region of high stress gradients. It can also cause less obvious problems related to the stress tensor symmetry, for example, $\sigma_{xy} = \sigma_{yx}$. Although all numerical and approximate analytical solutions assume that the stress tensor is symmetric, the moment equilibrium

equations of an infinitesimal volume element show that it can be unsymmetric if the first partial derivatives of stress are unbounded (see ref. 11, page 67 or ref. 12. page 40).

To illustrate the unsymmetry of the stress tensor at a point of a stress discontinuity, consider the problem of uniform pressure on part of a semi-infinite plane as shown in figure 3(a). The problem has an exact solution which may be readily derived from equations given in reference 13, page 127. The solution is as follows:

$$\left. \begin{aligned} \sigma_x &= -\frac{p}{\pi} \left\{ \arctan \left(\frac{y}{x-a} \right) + \frac{(x-a)y}{(x-a)^2 + y^2} - \arctan \left(\frac{y}{x+a} \right) - \frac{(x+a)y}{(x+a)^2 + y^2} \right\} \\ \sigma_y &= -\frac{p}{\pi} \left\{ \arctan \left(\frac{y}{x-a} \right) - \frac{(x-a)y}{(x-a)^2 + y^2} - \arctan \left(\frac{y}{x+a} \right) + \frac{(x+a)y}{(x+a)^2 + y^2} \right\} \\ \sigma_{xy} &= -\frac{p}{\pi} \left\{ \frac{y^2}{(x-a)^2 + y^2} - \frac{y^2}{(x+a)^2 + y^2} \right\} \end{aligned} \right\} \quad (2)$$

The boundary condition on the shear stress is that $\sigma_{yx} = 0$ along $y = 0$, which is satisfied by the above solution. However, if the points $(\pm a, 0)$ are approached along $x = \pm a$, then $\sigma_{xy}(\pm a, 0) = \mp p/\pi$. Therefore, $\sigma_{xy} \neq \sigma_{yx}$ at the points $(\pm a, 0)$ due to the stress discontinuity.

The exact solution was obtained using the Airy stress function which was developed from the equilibrium equations with $\sigma_{yx} = \sigma_{xy}$ at all interior points of the region. The only condition imposed on the solution at the boundary was that it satisfy the applied boundary conditions. Symmetry of the stress tensor at boundary points is not necessary for the Airy stress function to exist. Similar results of $\sigma_{xy} \neq \sigma_{yx}$ can be shown at singular points, for example, at the tip of a crack where the stresses are also unbounded.

The complete elasticity solution accounts for the proper behavior of the stress components everywhere in a continuum including the neighborhood of stress discontinuities and singularities. On the other hand, numerical and approximate analytical solutions allow considerable freedom in specifying the nature of the solution and significant errors can be introduced by enforcing incorrect symmetry conditions.

As mentioned earlier, numerical and approximate procedures are based on the assumption of a symmetric stress tensor everywhere in the continuum including the points with stress discontinuities and singularities. Therefore, these procedures cannot account for an unsymmetric stress tensor at these points, and this leads to difficulties. For example, in figure 3(a) prescription of the boundary condition $\sigma_{yx} = 0$ at $(\pm a, 0)$ automatically sets $\sigma_{xy} = 0$ at these

points. The numerical solutions obtained with those boundary conditions cannot, in general, agree with the exact solution.

In the displacement-based finite element analyses, the boundary conditions on stresses are not specified at discrete points. Rather, on parts of the boundary where stresses are prescribed, the boundary conditions are accounted for through equivalent nodal forces. The nodal forces represent integrals of the surface tractions. These integrals are always bounded whether or not a stress singularity or discontinuity exists. Therefore, it is of interest to study how the finite element method calculates the stresses near stress discontinuities or singularities.

FINITE ELEMENT ANALYSIS OF WELL-KNOWN PROBLEMS

In this section, finite element solutions for two well-known problems involving stress discontinuities and singularities are presented and compared with exact solutions. For each problem the relevant domain was idealized by eight-noded isoparametric elements. Three meshes - coarse, medium, and fine - were used. The medium mesh was obtained by subdividing each element of the coarse mesh into four elements. Similarly, the fine mesh was obtained by subdividing each element of the medium mesh into four elements.

Stress Discontinuity

Figure 3(a) shows a semi-infinite plate with a uniform pressure p over the region $-a \leq x \leq a$. As discussed in the previous section, stress discontinuities exist at the ends, A and A', of the loaded region. The exact solution for the problem is given in equation (2). Figure 3(b) shows the fine mesh idealization for the problem.

Figure 4 shows the normalized shear stress distribution σ_{yx} on the line $y = 0$, which should be zero. In this figure and all subsequent figures the fine mesh results are represented by a solid curve through the data; only the peak value is shown by a diamond symbol. The coarse and medium mesh results are shown by circular and rectangular symbols, respectively. The finite element stress for the three meshes is approximately zero except in the neighborhood of point A. Very near point A the shear stress σ_{yx} had relatively large positive and negative values. However, for all three meshes the nonzero values were confined to two elements on either side of point A. The integral of the shear stress $\int_0^{10a} \sigma_{yx} dx$ on the $y = 0$ line was nearly zero for all mesh refinements.

Figure 5 presents the normalized shear stress distribution σ_{xy} on the line $x = a$ for $0 \leq y \leq a$. The finite element solutions with the three meshes agreed very well with the exact solution except in the immediate neighborhood of point A. Again, the region of disagreement was confined to the two elements nearest the discontinuity. Numerical integration revealed that the equilibrium

condition $\int_0^{10a} \sigma_{xy}|_{x=a} dy = pa$ was satisfied approximately for all idealizations.

Stress Singularity

A bimetallic plate subjected to uniform tension was selected to illustrate finite element results near a singularity resulting from an interface between dissimilar materials. Figure 6(a) shows the plate with tension on the edges at $y = \pm 8a$, remote from the interface and with traction free sides along $x = 0$ and $x = 8a$. Stress singularities exist at points A and A' (refs. 14 and 15). The finite element idealization for a rigid bottom plate ($E^{II} = \infty$) is shown in figure 6(b).

The stresses on any radial line from the singular point A (or A') have the form (refs. 14 and 15)

$$\{\sigma\} = \{C\}r^{-\alpha} + O(r^{-\alpha+1}) \quad (3)$$

where $\{C\}$ is a vector of constants, r is the radial distance from point A and $O(r^{-\alpha+1})$ represents terms of the order $r^{-\alpha+1}$ and higher.

The exponent α is the singularity power. For the case of a rigid bottom plate ($E^{II} = \infty$), plane strain conditions and $\nu^I = 0.3$, the α has a value of 0.289.

As point A is approached along the bond line, $y = 0$, the shear stress σ_{yx} will be singular with $\alpha = 0.289$. But as point A is approached along the free edge, $x = 0$, the shear stress σ_{xy} has a zero value. Therefore, the shear stress and its complement are unequal at the singular point.

Figure 7 presents the normalized shear stress along the bond line, $y = 0$, obtained with the three meshes. Because of the singularity, the shear stress had a steep gradient very near $x/a = 0$. The shear stresses for the fine mesh were fitted to equation (3) and α was found to be 0.263. This value agrees well with the 0.289 obtained from references 14 and 15.

Figure 8 shows the normalized shear stress distribution along the $x = 0$ line. As expected, the shear stress was nearly zero all along the free edge and was nonzero only near the singular point. As in the stress discontinuity case, the regions of nonzero values were confined to two-element thicknesses. Numerical integration showed that the integral of the shear stress

$$\int_0^{8a} \sigma_{xy}|_{x=0} dy \text{ was nearly zero for all mesh refinements.}$$

These two examples suggest that the finite element solutions are accurate everywhere except very near a stress discontinuity or a singularity. However,

the region of inaccuracy is limited to about two elements and such a region can be made very small by progressive mesh refinement. Therefore, these examples indicate that valid results may be obtained by finite element methods in the neighborhood of singularities and discontinuities.

FINITE ELEMENT ANALYSIS OF THE EDGE-STRESS PROBLEM

As previously mentioned, the objective of the present study was to develop an accurate numerical solution for the edge-stress problem of a composite laminate. Attention was focused on a $[\pm 45]_S$ laminate. The finite element idealization for the $[\pm 45]_S$ laminate is presented first, followed by a convergence study of the stresses near the interface corner. Stress distributions are presented for the laminate interface and through the thickness at the free edge. Finally, equilibrium considerations are discussed.

Idealizations

Because of the symmetries in the problem, only the shaded region ($0 \leq y \leq b$; $0 \leq z \leq 2h$) in figure 1(b) of an $x = \text{Constant}$ plane was considered. The displacement functions U and V were prescribed as zero on the $y = 0$ line and the displacement function W was prescribed as zero on the $z = 0$ line.

The shaded region in figure 1(b) was idealized by eight-noded isoparametric elements as shown in figure 9. To study the convergence of the stresses near the free edge, three meshes were used. The medium mesh in figure 9(b) was obtained by subdividing each element of the coarse mesh (fig. 9(a)) into four elements. The fine mesh in figure 9(c) was obtained by a similar subdivision of each element of the medium mesh. The coarse mesh had 135 nodes and 36 elements, the medium mesh had 485 nodes and 144 elements, and the fine mesh had 1833 nodes and 576 elements.

Convergence Study

The stress distributions obtained with the three mesh models for a $[\pm 45]_S$ laminate were examined. The stresses that showed the steepest gradients were the interlaminar normal stress σ_z and the interlaminar shear stress σ_{xz} . The distributions for these stresses through the thickness at the face edge and along the interface are compared for the three models.

Interlaminar normal stress σ_z .— Figure 10(a) shows the σ_z distribution through the thickness along the free edge, $y = b$, for the three models. In this figure and all subsequent figures the fine mesh results are represented by a curve through the data; only the value at the interface is shown as a discrete value (diamond symbol). The coarse and medium mesh results are shown by circular and rectangular symbols, respectively. The solid symbols indicate the stresses in $+45^\circ$ ply. As shown on the figure, the values of σ_z for the three meshes agree closely except near the interface. At the interface, the three meshes produced noticeably different σ_z values but with the same sign.

Figure 10(b) shows the average interlaminar values of σ_z plotted against normalized distance from the free edge. The σ_z results from the three meshes are in excellent agreement for $(b - y)/h \geq 0.08$. However, at the free edge, $y = b$, due to the singularity, the computed σ_z values are again noticeably different for the three meshes, with the fine mesh producing the largest value.

Interlaminar shear stress σ_{xz} .— Figure 11(a) presents the through-the-thickness distributions of σ_{xz} at the free edge, $y = b$, for the three models. Figure 11(b) shows the σ_{xz} distributions along the interface. For all three meshes, as in figure 10, the computed stresses differed significantly only very near the interface corner, with the fine mesh again giving the largest values.

From these results it is evident that the finite element solution converges everywhere except very near the interface corner. That is, for decreasing mesh size, the computed stresses continue to change only in this particular region. This region is very small, on the order of $(b - y)/h < 0.08$ in figures 10 and 11. The stresses outside this region are believed to be accurate when interpreted in the light of the previous discussions for points near stress discontinuities and singularities.

Stress Distributions

Along the interface.— The stress distributions along the interface, $z = h$, obtained with the fine mesh model are presented in figure 12. For completeness, the σ_z and σ_{xz} results from figures 10 and 11 are also included. Figure 12(a) shows the σ_x , σ_y , σ_{xy} , and σ_{xz} distributions and figure 12(b) shows the σ_z and σ_{zy} distributions plotted against the normalized distance from the free edge. These stresses were computed from the elements in the $+45^\circ$ ply. The corresponding stresses in the -45° ply were nearly identical except the signs of σ_{xy} and σ_{zy} were reversed.

Figure 12 shows that σ_x , σ_y , and σ_{xy} attain the classical-laminate-theory values at a distance of about $4h$ from the free edge. The three dimensional stresses σ_z , σ_{zy} , and σ_{xz} all decay to zero at a similar distance from the edge. Near the edge, all stresses have gradients. The stresses σ_x , σ_y , and σ_{xy} increase near the edge but drop abruptly in the two elements nearest the edge. On the other hand, the shear stress σ_{zy} in figure 12(b) passes through zero and rises steeply to a positive peak at the edge. This sudden rise, once again, occurs in the two elements closest to the edge.

Because the interface corner is on the free edge, the stresses σ_y , σ_{xy} , and σ_{zy} should have a zero value. However, because a singularity exists at the interface corner (ref. 10) and because the finite element solution does not prescribe zero boundary stresses, these stresses have nonzero values. It is of interest, therefore, to examine the through-the-thickness distributions of σ_y , σ_{xy} , and σ_{zy} at the free edge.

Through the thickness.- Figures 13 to 15 show the distribution of σ_y , σ_{yx} , and σ_{yz} , respectively, in the top ply (+45°) along the free edge for all three mesh models. The stresses in the -45° ply were nearly identical to those of the +45° ply, except the σ_{yx} and σ_{yz} signs were reversed. Also included in figures 13 and 15 are the finite element results obtained with Wang and Crossman's (ref. 6) model. These results were obtained with three-noded triangular elements and, in general, lie between the present coarse and medium mesh results that were based on eight-noded isoparametric elements.

Figures 13 to 15 indicate that the stresses σ_y , σ_{yx} , and σ_{yz} were very nearly zero for most of the free edge. As in the previous examples, the region of disturbance was limited to two elements on either side of the interface. With progressive mesh refinement, the thickness of the elements was reduced and so was the region of disturbance. For all three stresses σ_y , σ_{yx} , and σ_{yz} (figs. 13, 14, and 15, respectively) numerical integration revealed that

$$\int_h^{2h} \sigma_y dz \qquad \int_h^{2h} \sigma_{yx} dz \qquad \int_h^{2h} \sigma_{yz} dz$$

were nearly zero for each of three models. However at the interface corner, each of the stresses σ_y , σ_{yx} , and σ_{yz} had nonzero values and, curiously, these values were unaffected by mesh refinements. In general, for a very fine mesh, these results indicate that the computed stresses would be zero all along the free edge except at the interface corner.

Because a stress singularity exists at the interface corner and recalling the results for the finite element solutions and the exact solutions in figures 4, 5, 7, and 8, this discrepancy of stresses on the boundary is expected near the interface corner.

Equilibrium Considerations

Any solution to the edge-stress problem should satisfy the following equilibrium requirements. As shown in figure 16, the top ply of a $[\pm 45]_S$ can be treated as a free body. Equilibrium requirements for the free body are

y-force equilibrium

$$\int_h^{2h} \sigma_y dz = \int_0^b \sigma_{yz} dy \qquad (4a)$$

z-force equilibrium

$$\int_0^b \sigma_z dy = 0 \quad (4b)$$

Moment equilibrium about (0,h)

$$\int_h^{2h} \sigma_y(z - h) dz = \int_0^b \sigma_{zy} dy \quad (4c)$$

For the $[\pm 45]_S$, the classical laminate theory predicts σ_y as zero in the interior of the laminate. Therefore, equations (4) reduce to

$$\int_0^b \sigma_{yz} dy = \int_0^b \sigma_z dy = \int_0^b \sigma_{zy} dy = 0 \quad (5)$$

Numerical integration of the stresses in figure 12(b) revealed that the present solution satisfies equations (5). However, it appears from figure 3 of reference 1 that the σ_z distributions obtained by finite difference techniques did not satisfy the last of equations (5). This is because the σ_z distributions changed sign only once, leaving an unbalanced moment. In the present finite element solution, σ_z changed from compression to tension at about $(b - y)/h = 0.2$ and changed sign again at about $(b - y)/h = 2.4$ before the stress σ_z became zero. This distribution left no unbalanced moment. The finite element results of reference 6 show similar behavior.

DISCUSSION OF NUMERICAL METHODS

Finite difference (refs. 1 and 3), perturbation (ref. 5), and finite element (refs. 6, 8, and 10) are all approximate methods which use the basic assumption of a symmetric stress tensor in their formulations. All along the free edge, including the interface corner, the finite difference and perturbation methods imposed the boundary conditions $\sigma_y = \sigma_{yx} = \sigma_{yz} = 0$. These boundary conditions force the complementary shear stresses σ_{xy} and σ_{zy} to also be zero at the interface corner. But at the interface corner, the stresses are singular and the stress tensor is not symmetric. Thus, the stresses σ_{xy} and σ_{zy} are not zero at the interface corner. If σ_y and σ_{xy} are zero,

it can be shown that σ_z is forced to be tensile for a tensile applied load. Details are given in the appendix. This may be the reason that the finite difference and perturbation methods predicted a tensile σ_z at the interface corner in figure 2.

On the other hand, the present finite element solution did not explicitly prescribe σ_y , σ_{yx} , and σ_{yz} to be zero at the interface corner. Instead it prescribed the normal and tangential forces on each of the element sides, which lie along the free edge, to be zero. Also, as discussed earlier, the integrals of the stresses σ_y , σ_{yx} , and σ_{yz} were zero in the present solution over the entire free edge, $y = b$. This shows that there were no net normal and tangential forces on the free edge. Furthermore, the finite element solution satisfied all equilibrium requirements.

CONCLUDING REMARKS

The edge-stress problem for a $[\pm 45]_S$ laminate has been studied by several investigators using finite difference, perturbation, and finite element displacement methods. The interlaminar normal stress σ_z distributions along the interface (between the $+45^\circ$ ply and the -45° ply) disagree in magnitude and sign for different methods. Because a stress singularity exists at the intersection of the interface and the free edge, the differences in magnitude of σ_z were expected. The difference in sign was not expected. The finite difference and perturbation techniques predicted a tensile σ_z , where as the finite element solutions predicted a compressive σ_z very near the free edge.

Available continuum solutions revealed that the stress tensor may not necessarily be symmetric (that is, $\sigma_{ij} \neq \sigma_{ji}$ for $i \neq j$) at a stress discontinuity or singularity. However, all approximate and numerical methods use symmetric stress tensors in their formulations. Therefore, two well-known problems, one involving a stress discontinuity and one a singularity, were analyzed to check the finite element method. These analyses showed that the finite element method yielded accurate solutions everywhere except in a region involving the two elements closest to the stress discontinuity or singularity, and that this region can be made arbitrarily small by refining the finite element model.

For the present analysis of a $[\pm 45]_S$ laminate, the finite element results near the singularity (at the intersection of the interface and the free edge) were similar to the behavior for the two well-known problems. The present finite element solutions for the edge-stress problem are, therefore, believed to be accurate except in the two elements closest to the singularity. Therefore, the present finite element displacement method, based on the total potential energy formulation, appears to be an accurate and useful technique for analyzing the edge stresses in a composite laminate.

The present finite element analysis of a $[\pm 45]_S$ laminate showed that the interlaminar stress σ_z is compressive at the intersection of the interface and the free edge. The finite difference and perturbation solutions in the literature may have predicted an incorrect sign (tensile) for the σ_z stress because of the assumption of a symmetric stress tensor combined with stress boundary conditions at the singular point.

Langley Research Center
National Aeronautics and Space Administration
Hampton, VA 23665
October 27, 1980

APPENDIX

POINT SOLUTION

In this appendix, a point solution is presented for the interlaminar normal stress σ_z at the interface corner of a $[\pm 45]_S$ laminate. A symmetric stress tensor and stress boundary conditions were assumed. This solution demonstrates that the magnitude and sign of σ_z at the interface corner can be explicitly obtained from the constitutive relations, continuity conditions along the interface, and the boundary conditions $\sigma_y = \sigma_{yx} = 0$.

Consider a $[\pm 45]_S$ laminate. The constitutive relations for a $+45^\circ$ ply are

$$\{\epsilon\} = [S]\{\sigma\} \quad (A1)$$

where

$$\{\epsilon\}^T = (\epsilon_x, \epsilon_y, \epsilon_z, \epsilon_{xy}, \epsilon_{yz}, \epsilon_{zx})$$

$$\{\sigma\}^T = (\sigma_x, \sigma_y, \sigma_z, \sigma_{xy}, \sigma_{yz}, \sigma_{zx})$$

and

$$[S] = \begin{bmatrix} S_{11} & S_{12} & S_{13} & S_{14} & 0 & 0 \\ & S_{22} & S_{23} & S_{24} & 0 & 0 \\ & & S_{33} & S_{34} & 0 & 0 \\ & & & S_{44} & 0 & 0 \\ \text{SYM.} & & & & S_{55} & 0 \\ & & & & & S_{66} \end{bmatrix}$$

Implicit in equation (A1) is the assumption of a symmetric stress tensor.

The stress-free boundary conditions along $y = b$ are

$$\sigma_y = \sigma_{yz} = \sigma_{yx} = 0 \quad (A2)$$

APPENDIX

Continuity of displacements along the interface, for all y , requires

$$\epsilon_{xy}^{45} = \epsilon_{xy}^{-45} \quad (A3)$$

and

$$\epsilon_Y^{45} = \epsilon_Y^{-45} \quad (A4)$$

The imposed axial strain is

$$\epsilon_x = \epsilon_0 \quad (A5)$$

Equations (A1), (A2), (A4), and the continuity of σ_z across the interface can be solved to show the stress σ_x in each of the 45° and -45° plies is the same. Solving equations (A1) to (A5) for the point where an interface meets the free edge gives

$$\left. \begin{aligned} \epsilon_0 &= S_{11}\sigma_x + S_{13}\sigma_z \\ 0 &= S_{14}\sigma_x + S_{34}\sigma_z \end{aligned} \right\} \quad (A6)$$

Solving equations (A6) for σ_x and σ_z ,

$$\left. \begin{aligned} \sigma_x &= \frac{\epsilon_0 S_{34}}{S_{11}S_{34} - S_{14}S_{13}} \\ \sigma_z &= \frac{-S_{14}}{S_{34}} \sigma_x \end{aligned} \right\} \quad (A7)$$

For graphite/epoxy laminates considered in this paper, equations (A7) give

$$\sigma_x = 24.62 \times 10^3 \epsilon_0 \text{ MPa}$$

$$\sigma_z = 57.44 \times 10^3 \epsilon_0 \text{ MPa}$$

Thus the point solution predicts a tensile σ_z at the interface corner for tensile applied strain as the finite difference and perturbation solutions predicted. Therefore, σ_z is forced to be tensile if a symmetric stress tensor is assumed and the boundary conditions $\sigma_y = \sigma_{yx} = \sigma_{yz} = 0$ are prescribed.

REFERENCES

1. Pipes, R. Byron; and Pagano, N. J.: Interlaminar Stresses in Composite Laminates Under Uniform Axial Extension. *J. Compos. Mater.*, vol. 4, Oct. 1970, pp. 538-548.
2. Rybicki, E. F.: Approximate Three-Dimensional Solutions for Symmetric Laminates Under Inplane Loading. *J. Compos. Mater.*, vol. 5, July 1971, pp. 354-360.
3. Pipes, R. B.: Interlaminar Stresses in Composite Laminates. AFML-TR-72-18, U.S. Air Force, May 1972. (Available from DTIC as AD 776 053.)
4. Tang, S.; and Levy, A.: A Boundary Layer Theory - Part II: Extension of Laminated Finite Strip. *J. Compos. Mater.*, vol. 9, Jan. 1975, pp. 42-52.
5. Hsu, Peter W.; and Herakovich, Carl T.: Edge Effects in Angle-Ply Composite Laminates. *J. Compos. Mater.*, vol. 11, Oct. 1977, pp. 422-428.
6. Wang, A. S. D.; and Crossman, Frank W.: Some New Results on Edge Effect in Symmetric Composite Laminates. *J. Compos. Mater.*, vol. 11, Jan. 1977, pp. 92-106.
7. Wang, James T. S.; and Dickson, John N.: Interlaminar Stresses in Symmetric Composite Laminates. *J. Compos. Mater.*, vol. 12, Oct. 1978, pp. 390-402.
8. Herakovich, C. T.; Nagarkar, A.; and O'Brien, D. A.: Failure Analysis of Composite Laminates With Free Edges. *Modern Developments in Composite Materials and Structures*, J. R. Vinson, ed., American Soc. Mech. Eng., 1979, pp. 53-66.
9. Spilker, Robert L.; and Chou, S. C.: Edge Effects in Symmetric Composite Laminates: Importance of Satisfying the Traction-Free-Edge Condition. *J. Compos. Mater.*, vol. 14, Jan. 1980, pp. 2-20.
10. Raju, I. S.; and Crews, J. H., Jr.: Interlaminar Stress Singularities at a Straight Free Edge in Composite Laminates. NASA TM-81876, 1980 .
11. Fung, Y. C.: *Foundations of Solid Mechanics*. Prentice-Hall, Inc., c.1965.
12. Sokolnikoff, I. S.: *Mathematical Theory of Elasticity*. Second ed. McGraw-Hill Book Co., Inc., 1956.
13. Timoshenko, S.; and Goodier, J. N.: *Theory of Elasticity*. Second ed. McGraw-Hill Book Co., Inc., 1951.
14. Williams, M. L.: Stress Singularities Resulting From Various Boundary Conditions in Angular Corners of Plates in Extension. *J. Appl. Mech.*, vol. 19, no. 4, Dec. 1952, pp. 526-528.
15. Hein, V. L.; and Erdogan, F.: Stress Singularities in a Two-Material Wedge. *Int. J. Fract. Mech.*, vol. 7, no. 3, Sept. 1971, pp. 317-330.

TABLE I.- SUMMARY OF INVESTIGATIONS FOR THE EDGE-STRESS PROBLEM

Investigator (s)	Reference	Method used	Laminate(s) analyzed
Pipes and Pagano	1	Finite difference	$[\pm 45]_s$
Rybicki	2	Finite element	$[\pm 45]_s, [0/90]_s, [90/0]_s$
Pipes	3	Finite difference	$[0/90]_s, [90/0]_s, [0/\pm 45]_s,$ $[\pm 45/0]_s, [45/0/-45]_s$
Tang and Levy	4	Boundary-layer theory	$[\pm \beta]_s, [\mp \beta]_s$
Hsu and Herakovich	5	Perturbation	$[\pm 45]_s$
Wang and Crossman	a ₆	Finite element	$[0/90]_s, [90/0]_s, [\pm 45]_s, Q \cdot I^b$
Wang and Dickson	7	Series solution	$[0/90]_s, [90/0]_s, Q \cdot I^b$
Herakovich et al.	a ₈	Finite element	$[0/90]_s, [90/0]_s, [\pm 45]_s, Q \cdot I^b$
Spilker and Chou	9	Hybrid stress Finite element	$[0/90]_s, [90/0]_s$
Raju and Crews	c ₁₀	Finite element	$[\theta/(\theta - 90)]_s; 0 \leq \theta \leq 90$

^aDisplacement-formulated finite element method with three-noded triangular elements.

^bQuasi-isotropic laminates, $[\pm 45/0/90]_s$ with several stacking sequences.

^cDisplacement-formulated finite element method with eight-noded isoparametric elements.

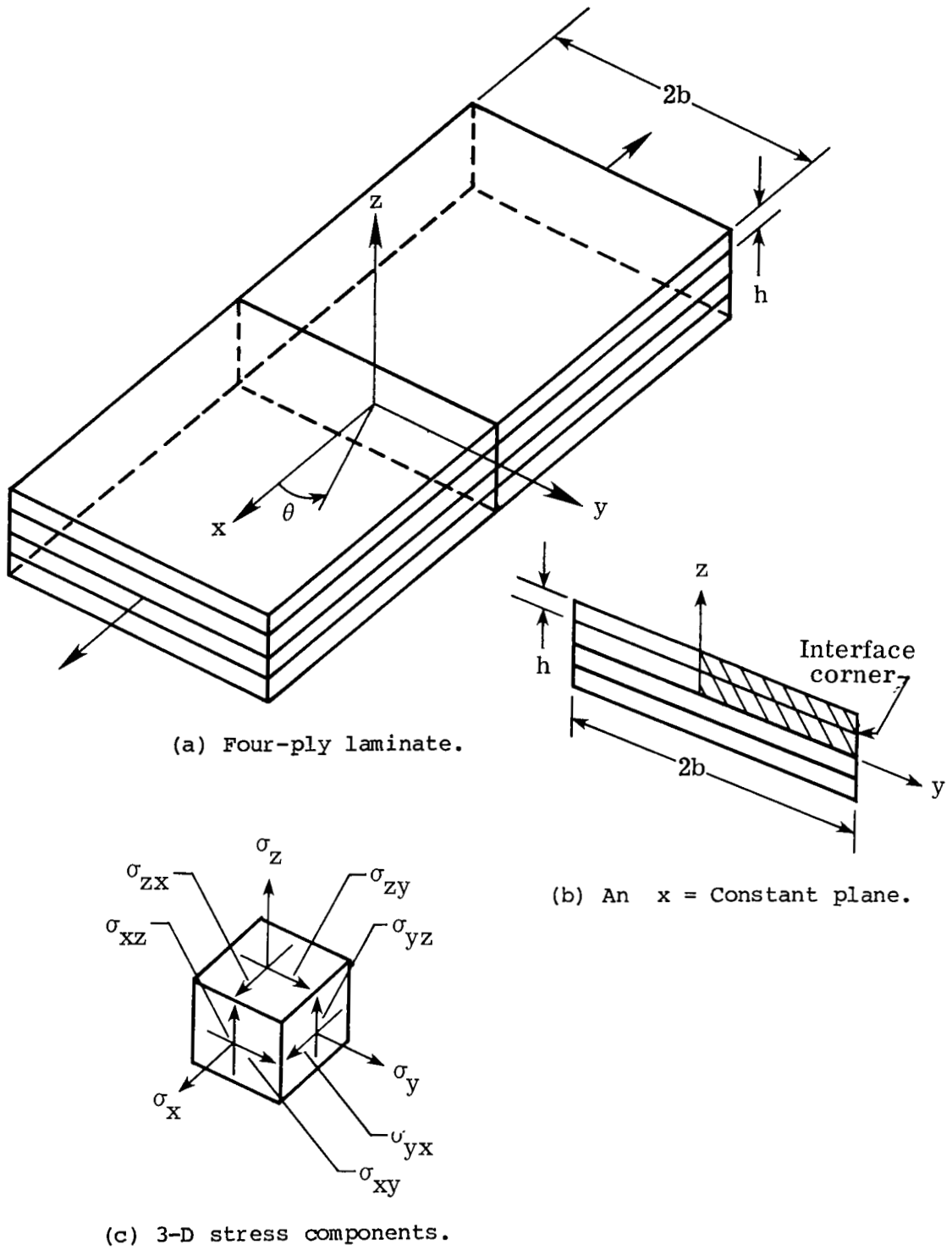


Figure 1.- Laminate configuration, loading, and stresses.

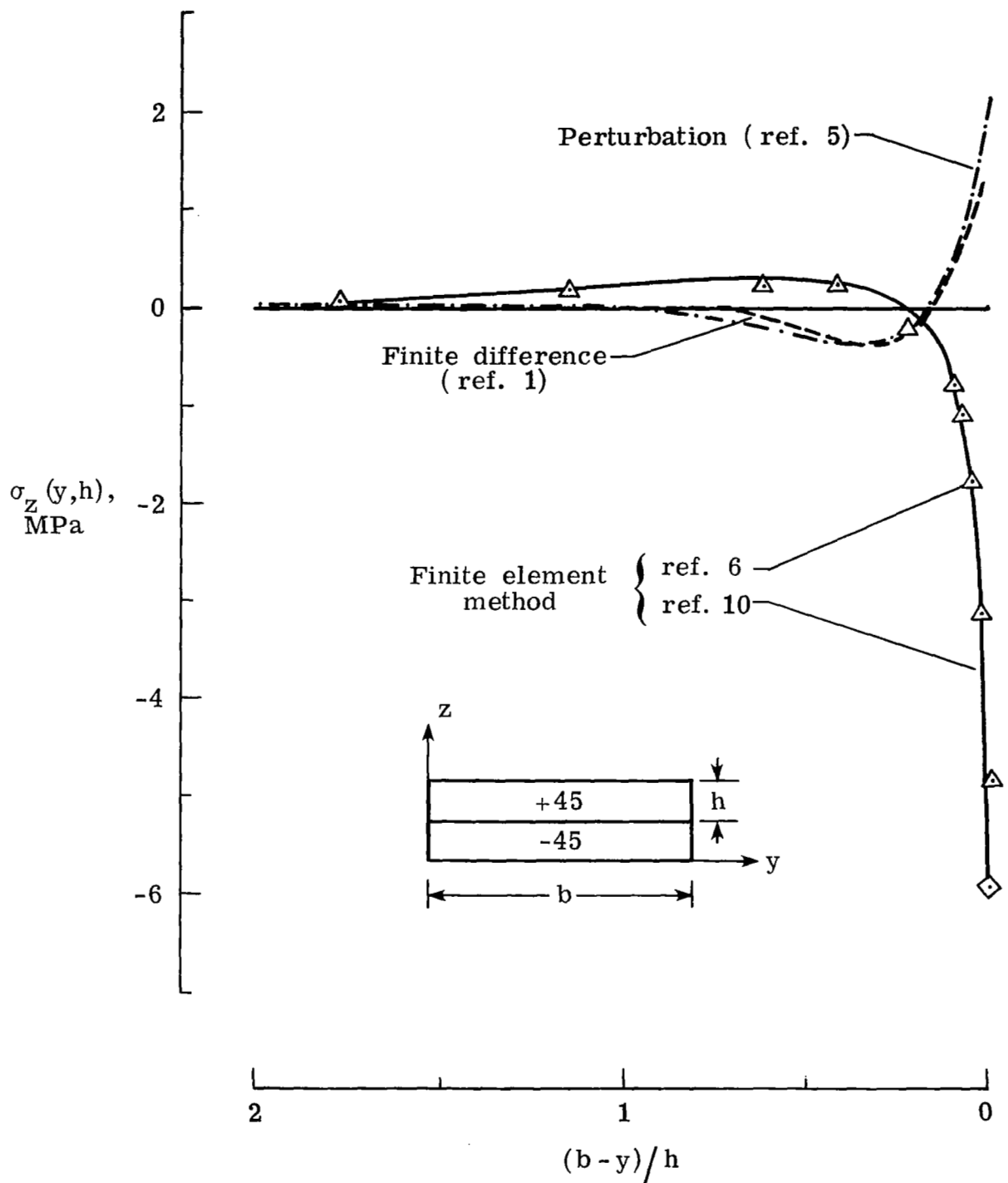
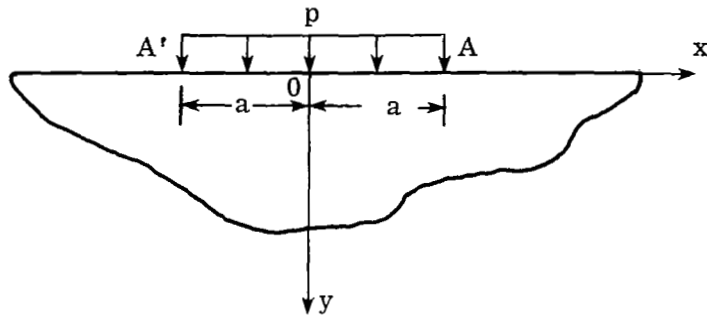
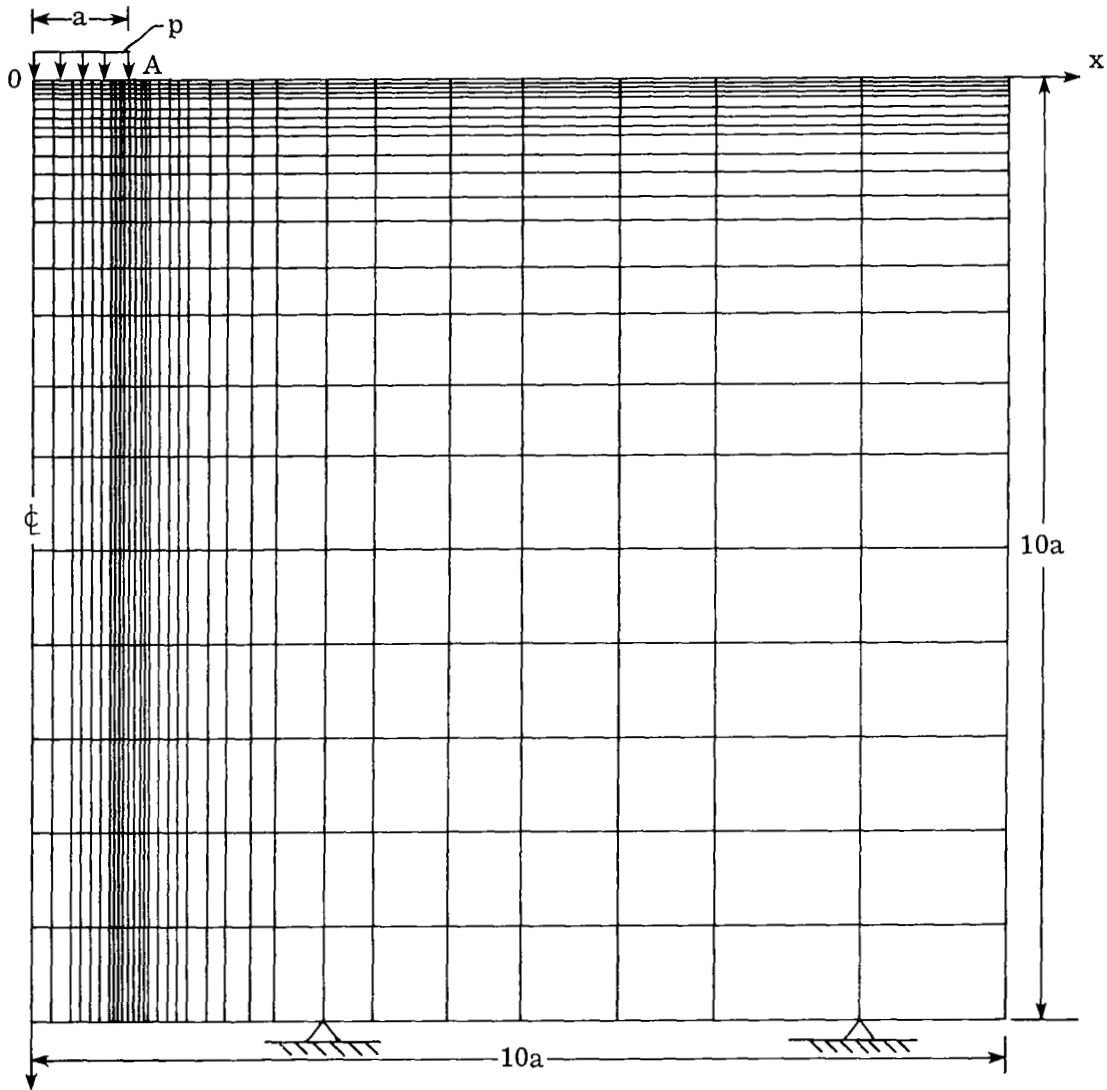


Figure 2.- Comparison of interlaminar normal stress calculated by various methods.



(a) Uniform load on a semi-infinite plate.



(b) Finite element idealization - fine mesh.

Figure 3.- Problem involving stress discontinuity.

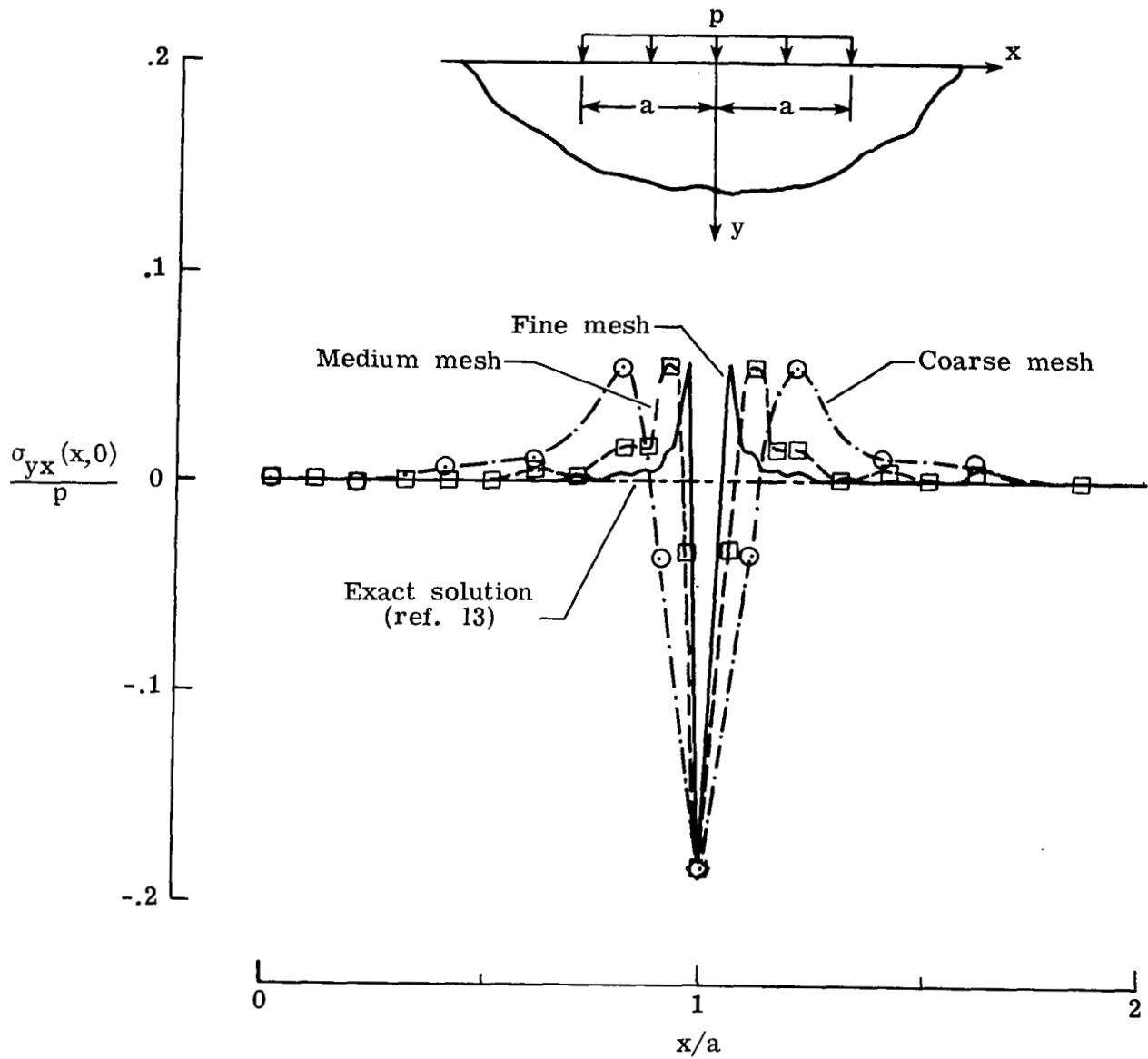


Figure 4.- Shear stress (σ_{yx}/p) distribution on $y = 0$ line.

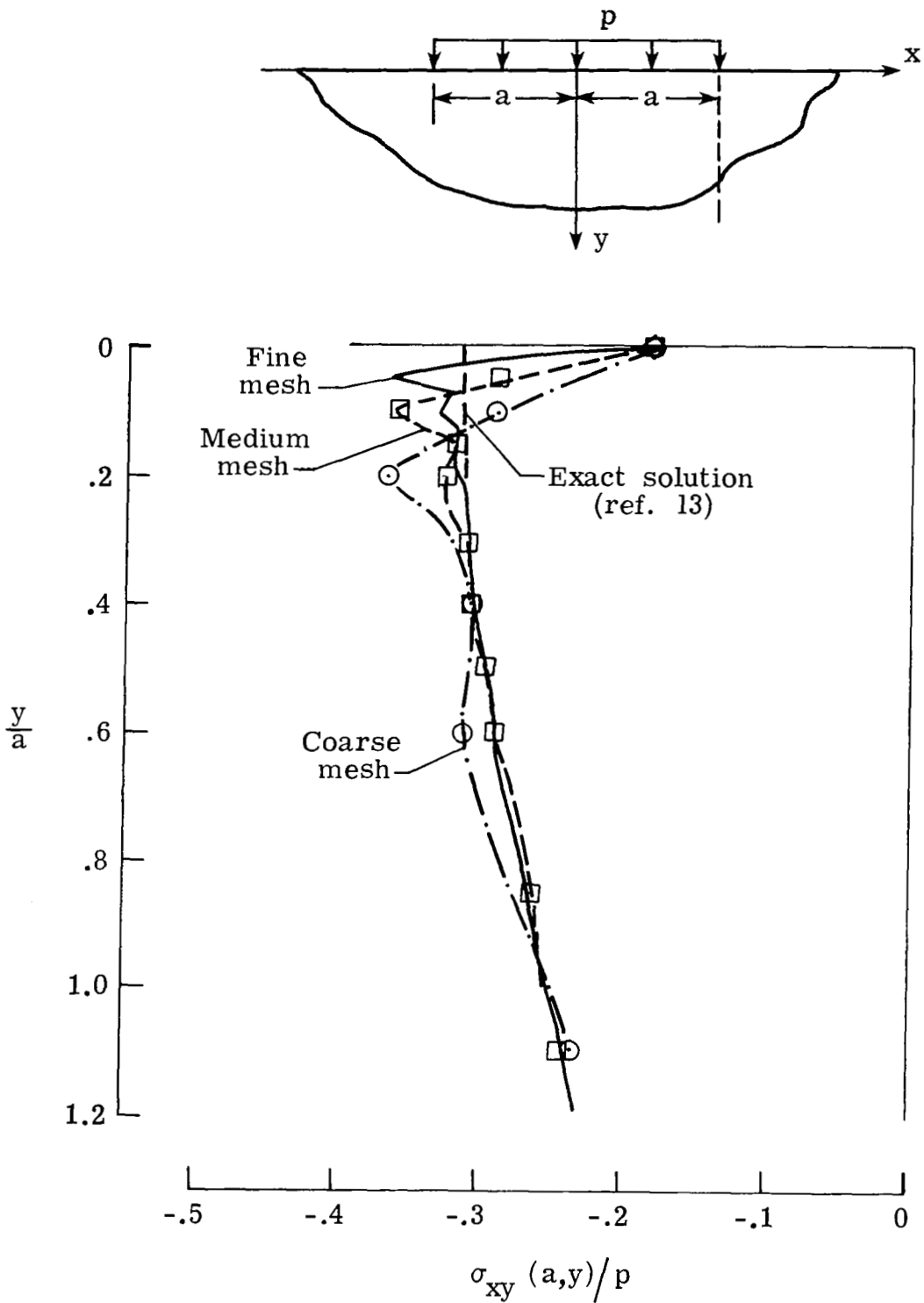
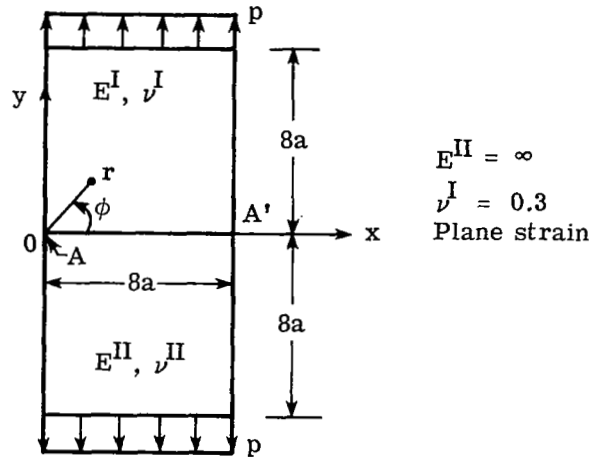
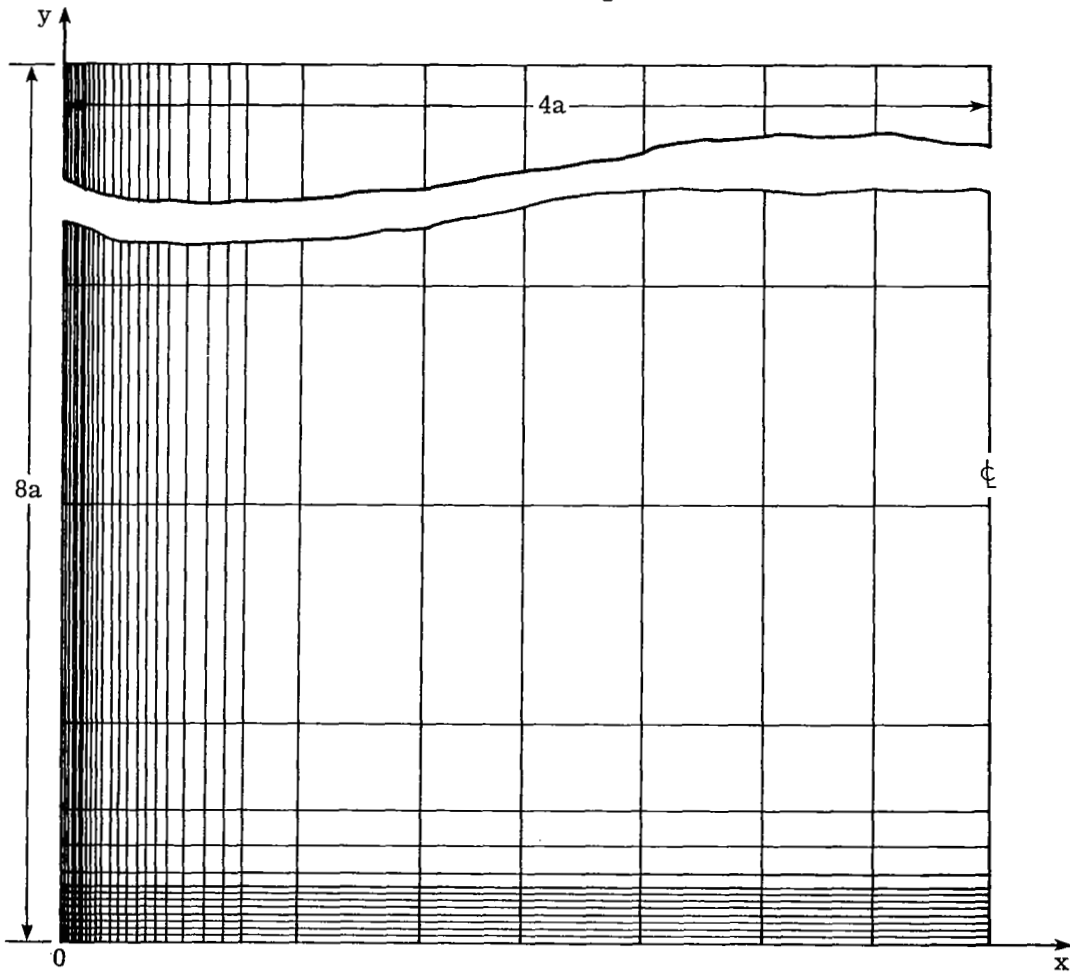


Figure 5.- Shear stress (σ_{xy}/p) distribution on $x = a$ line.



(a) An isotropic bimetallic plate under tension.



(b) Finite element idealization - fine mesh.

Figure 6.- Problem involving stress singularity.

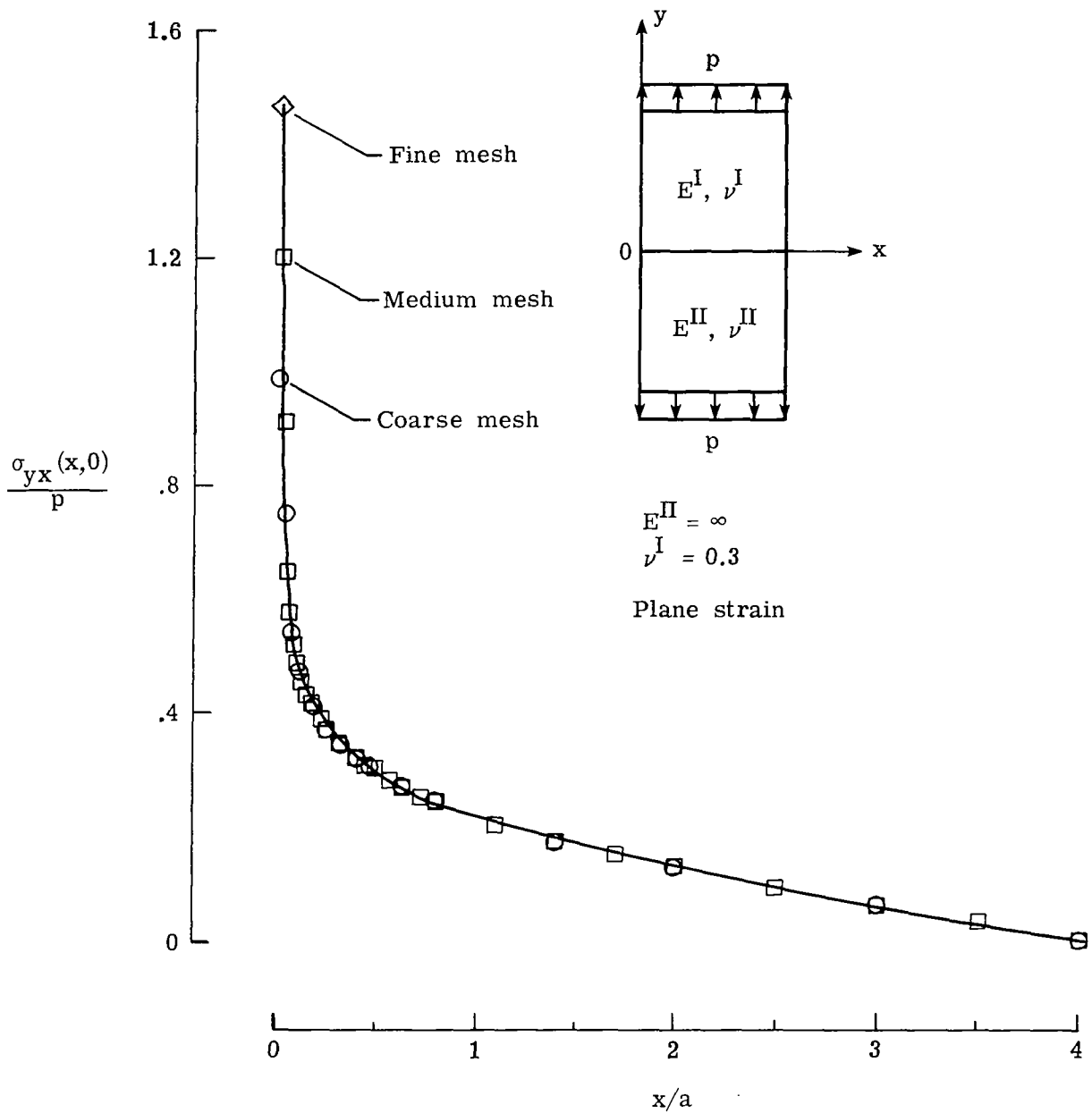


Figure 7.- Shear stress (σ_{yx}/p) distribution along the bond line ($y = 0$).

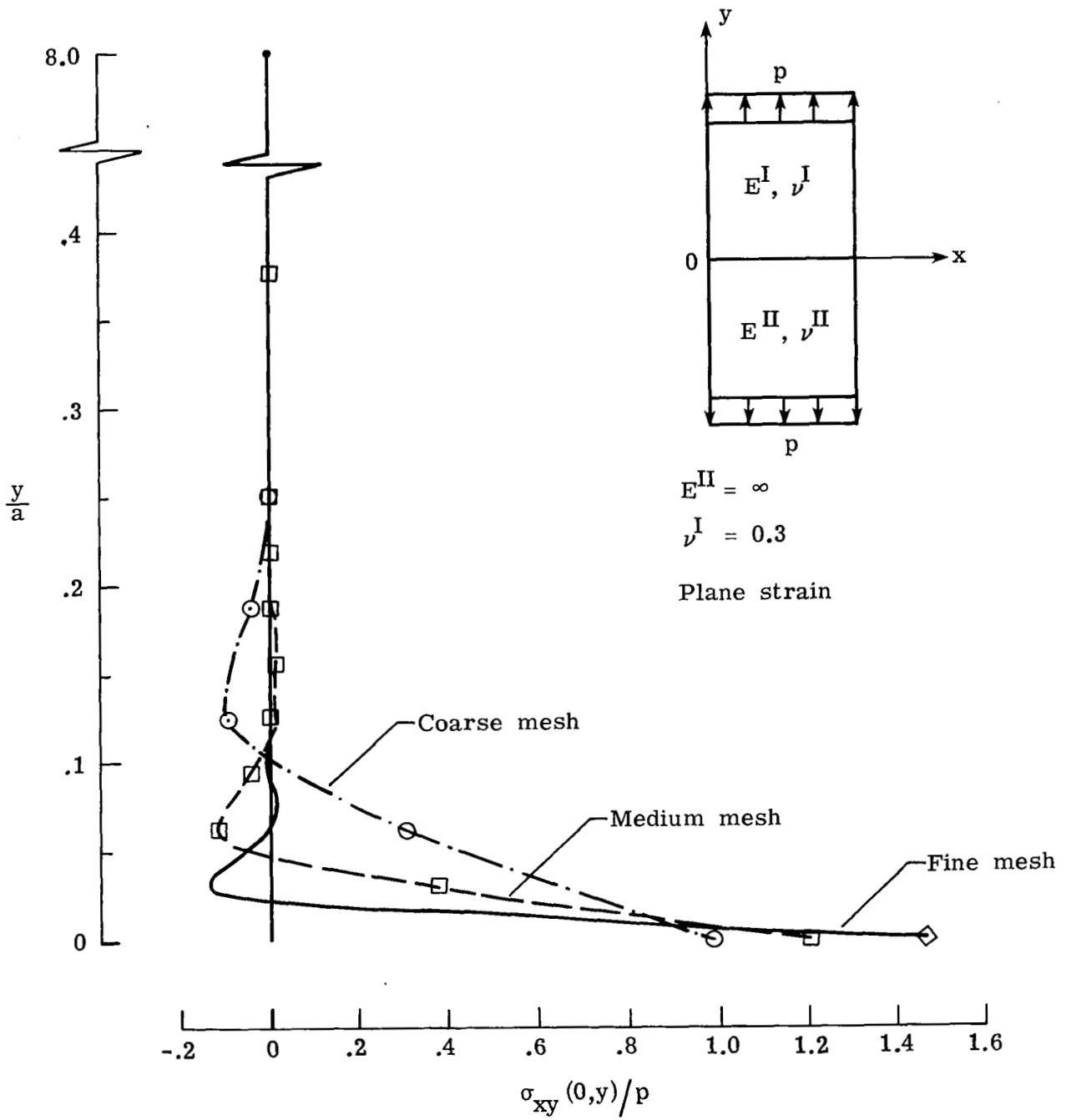
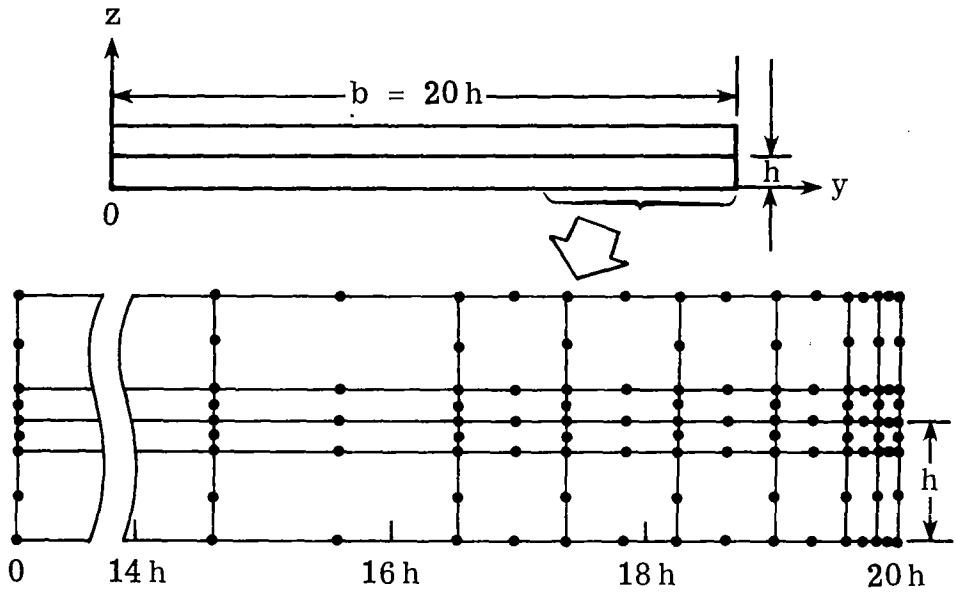
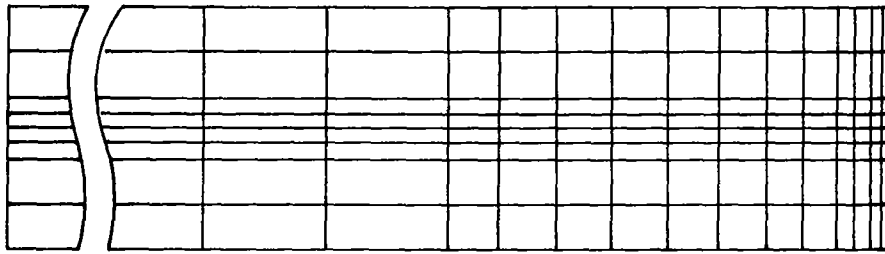


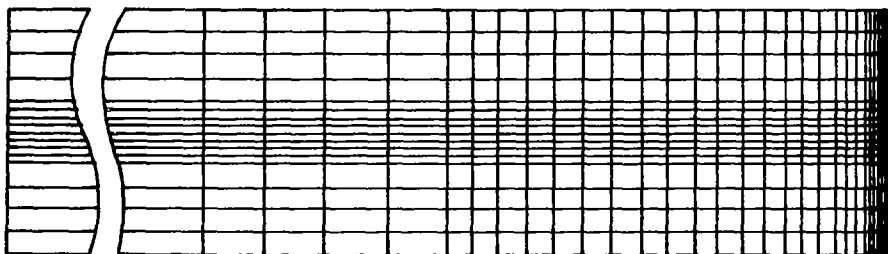
Figure 8.- Shear stress (σ_{xy}/p) distribution along the $x = 0$ line.



(a) Coarse mesh.

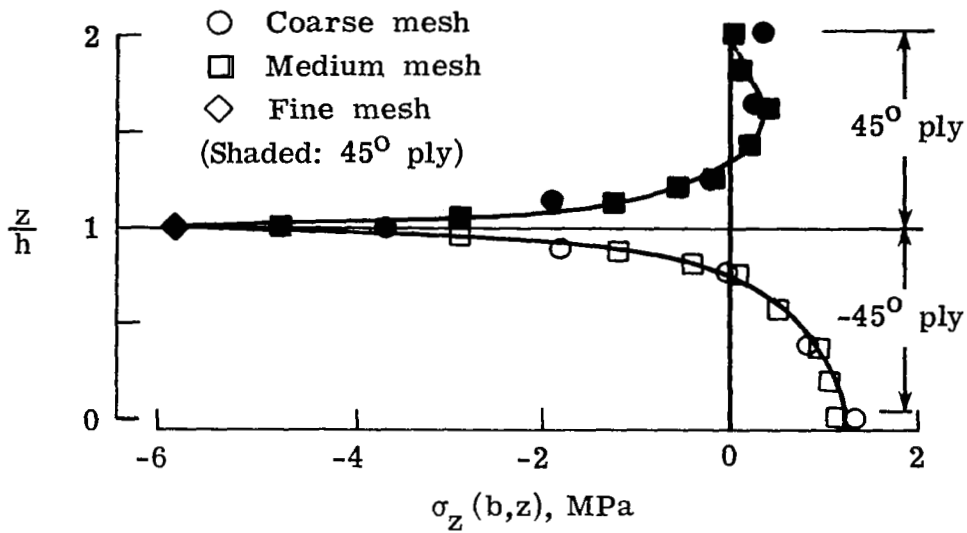


(b) Medium mesh.

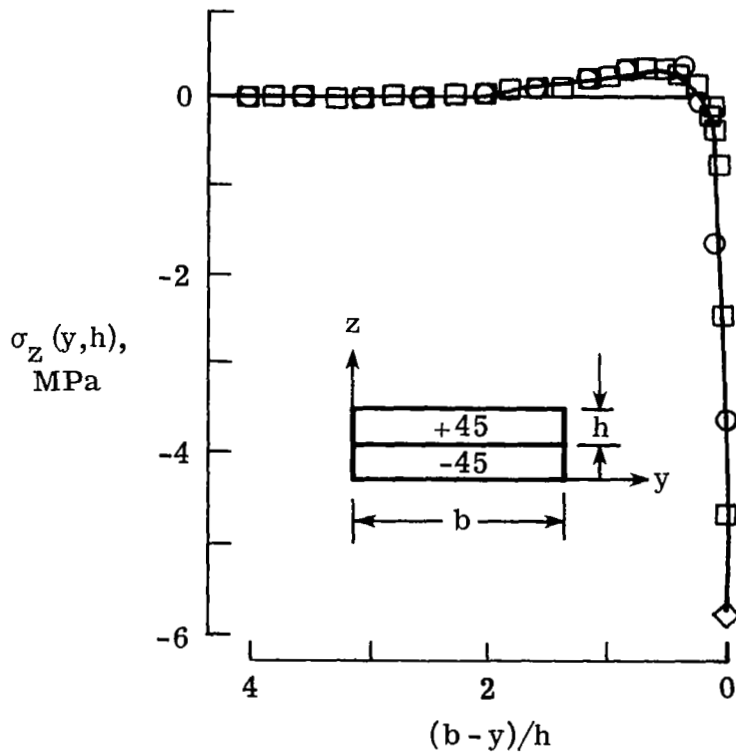


(c) Fine mesh.

Figure 9.- Rectangular mesh models.

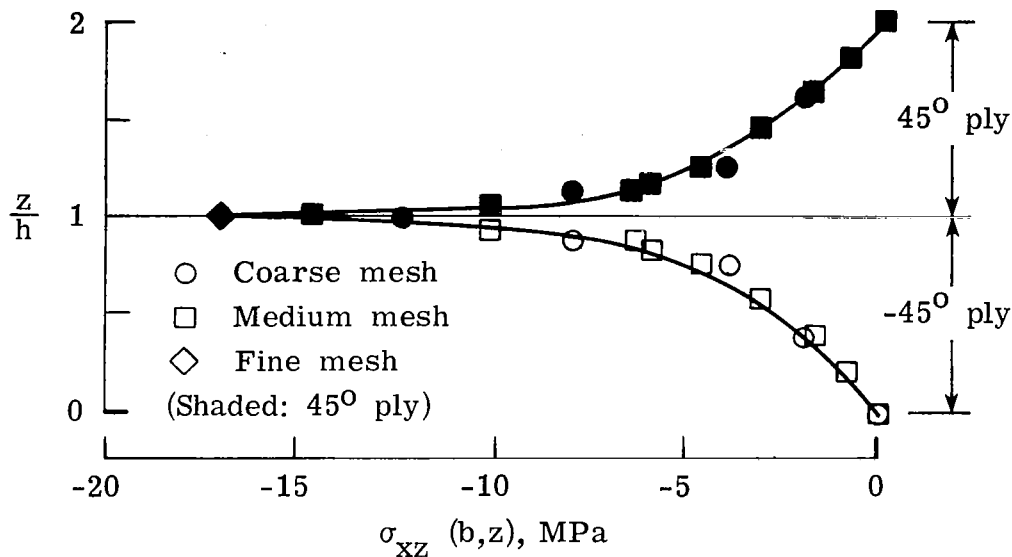


(a) σ_z along the free edge, $y = b$.

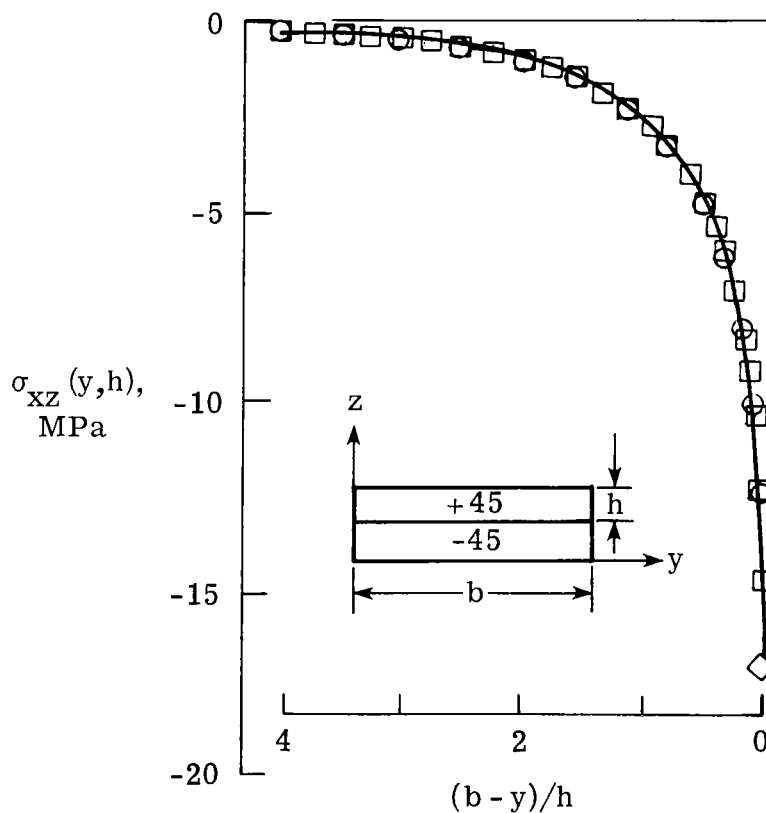


(b) σ_z along the interface, $z = h$.

Figure 10.- The σ_z distributions for various idealizations of a $[\pm 45]_S$ laminate.

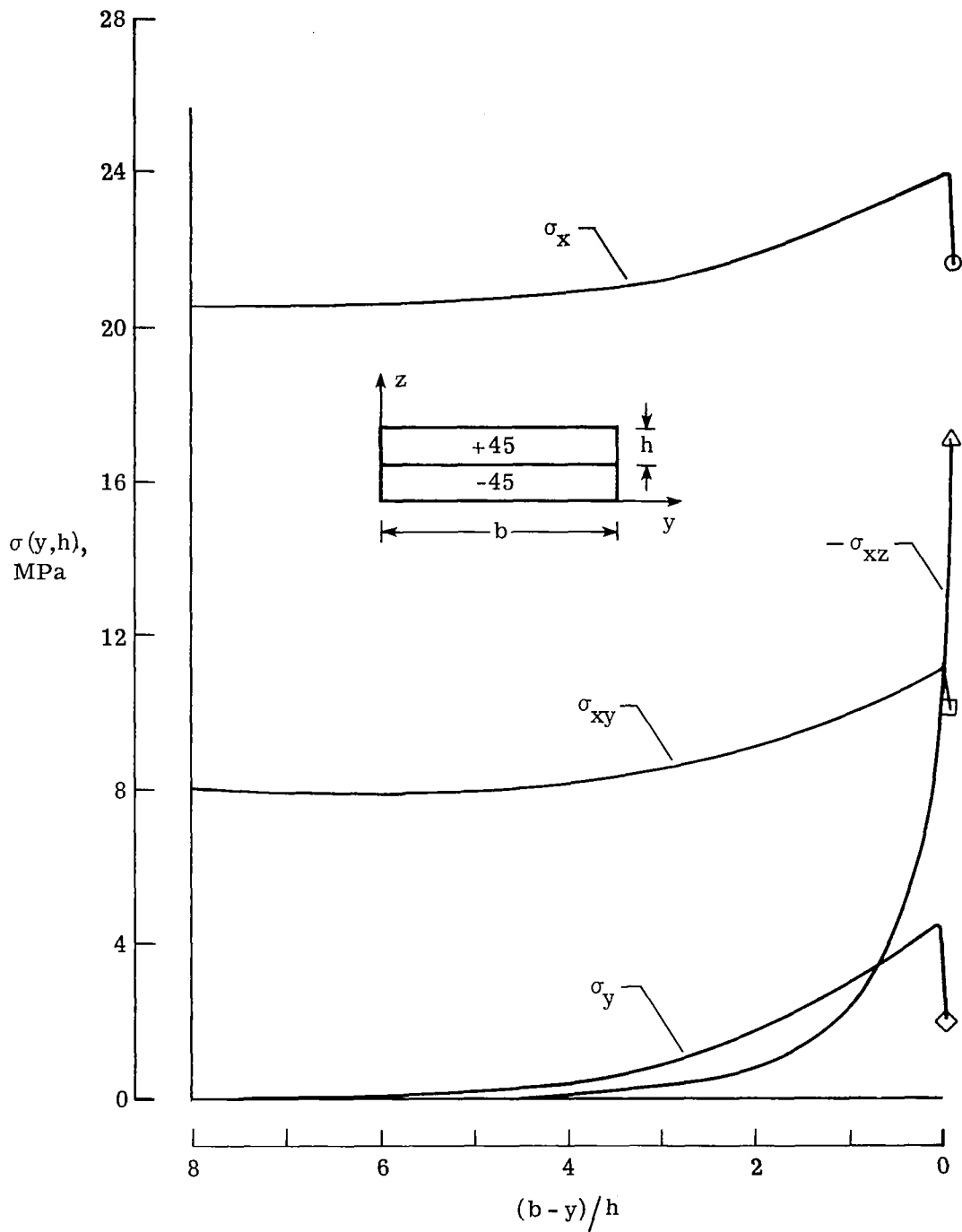


(a) σ_{xz} along the free edge, $y = b$.



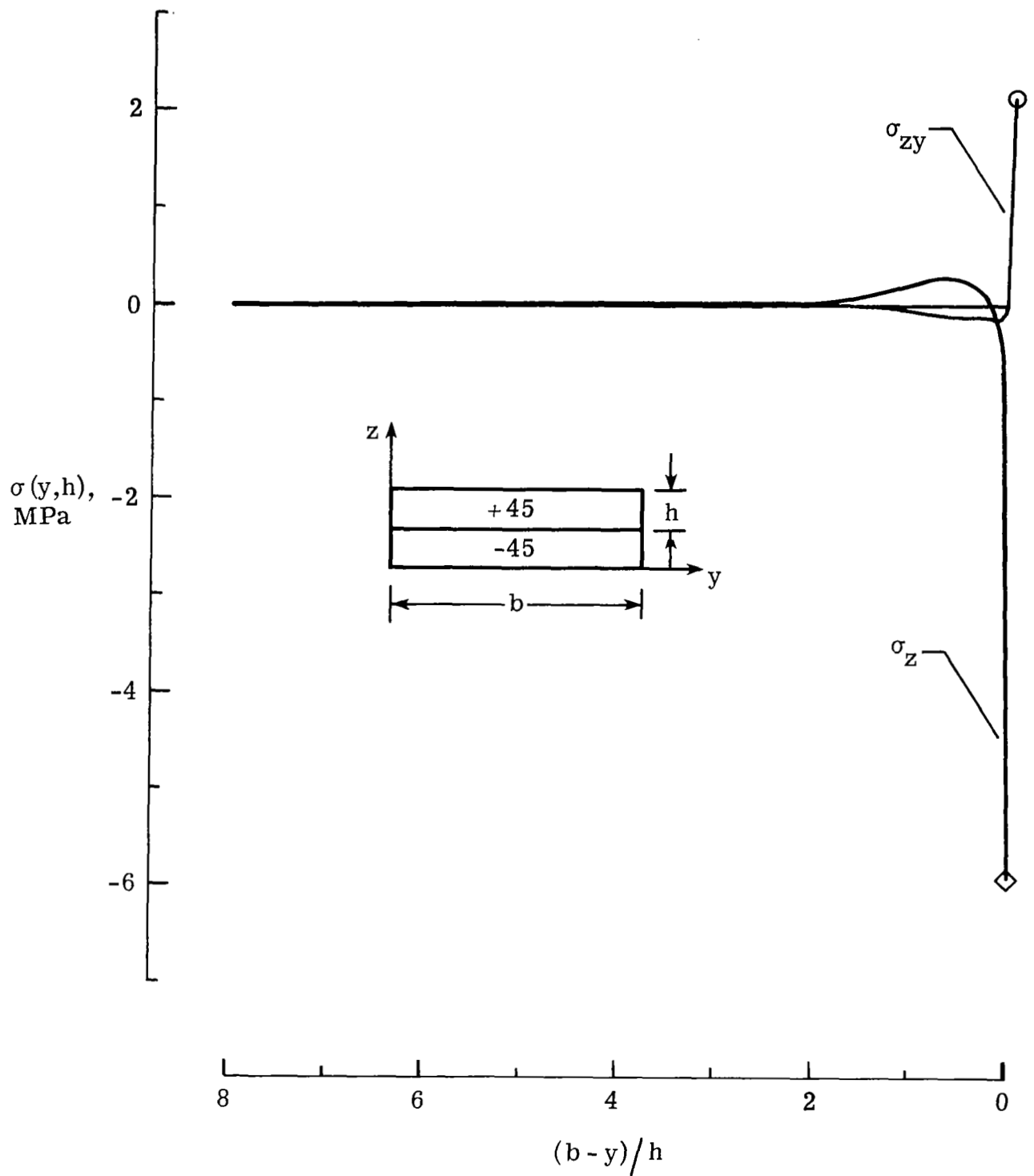
(b) σ_{xz} along the interface, $z = h$.

Figure 11.- The σ_{xz} distributions for various idealizations of the $[\pm 45]_S$ laminate.



(a) The σ_x , σ_y , σ_{xy} , and σ_{xz} distributions along the interface.

Figure 12.- Stress distributions along the interface, fine mesh.



(b) The σ_z and σ_{zy} distributions along the interface.

Figure 12.- Concluded.

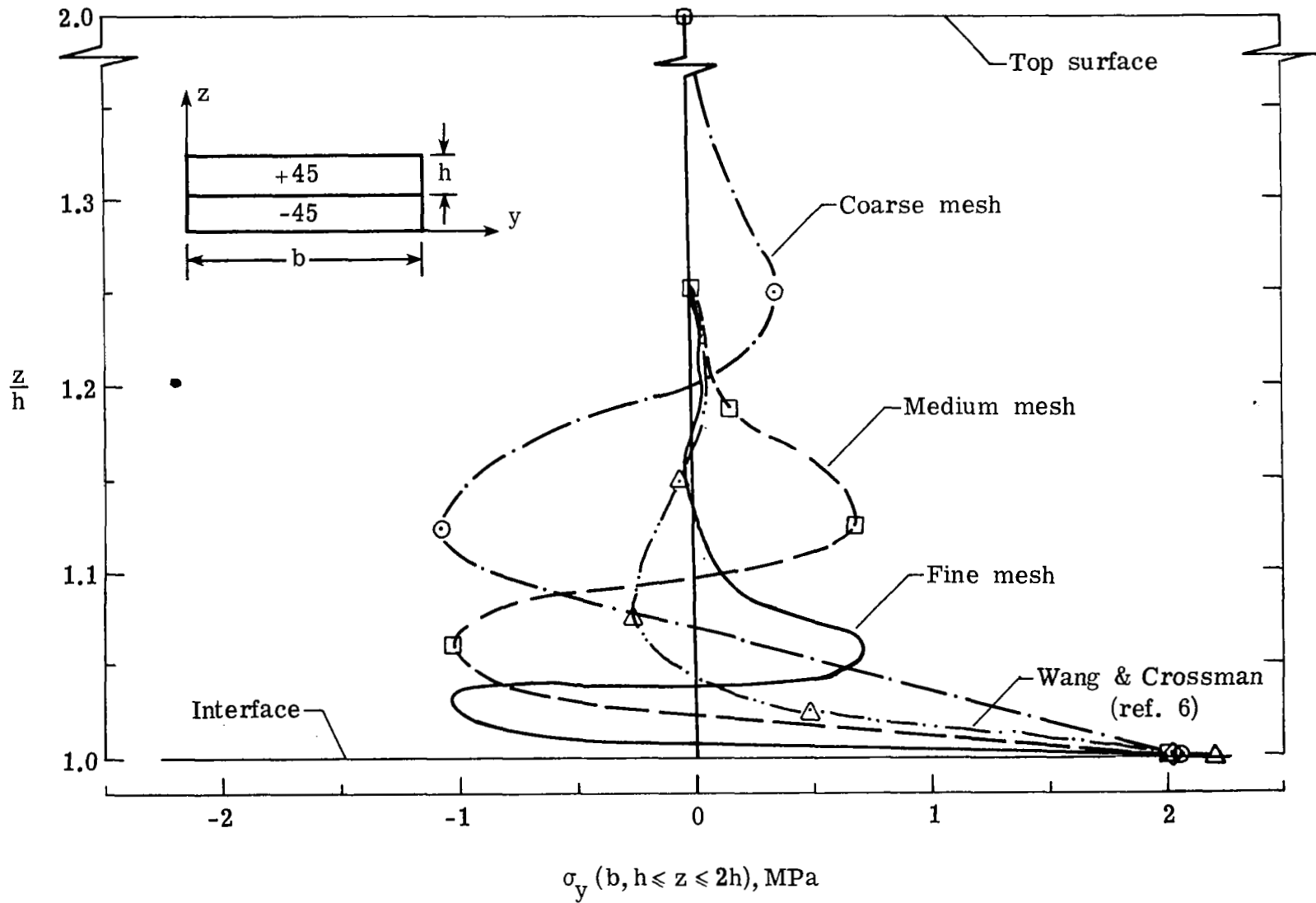


Figure 13.- Distribution of σ_y through the thickness at the free edge in the +45 ply.

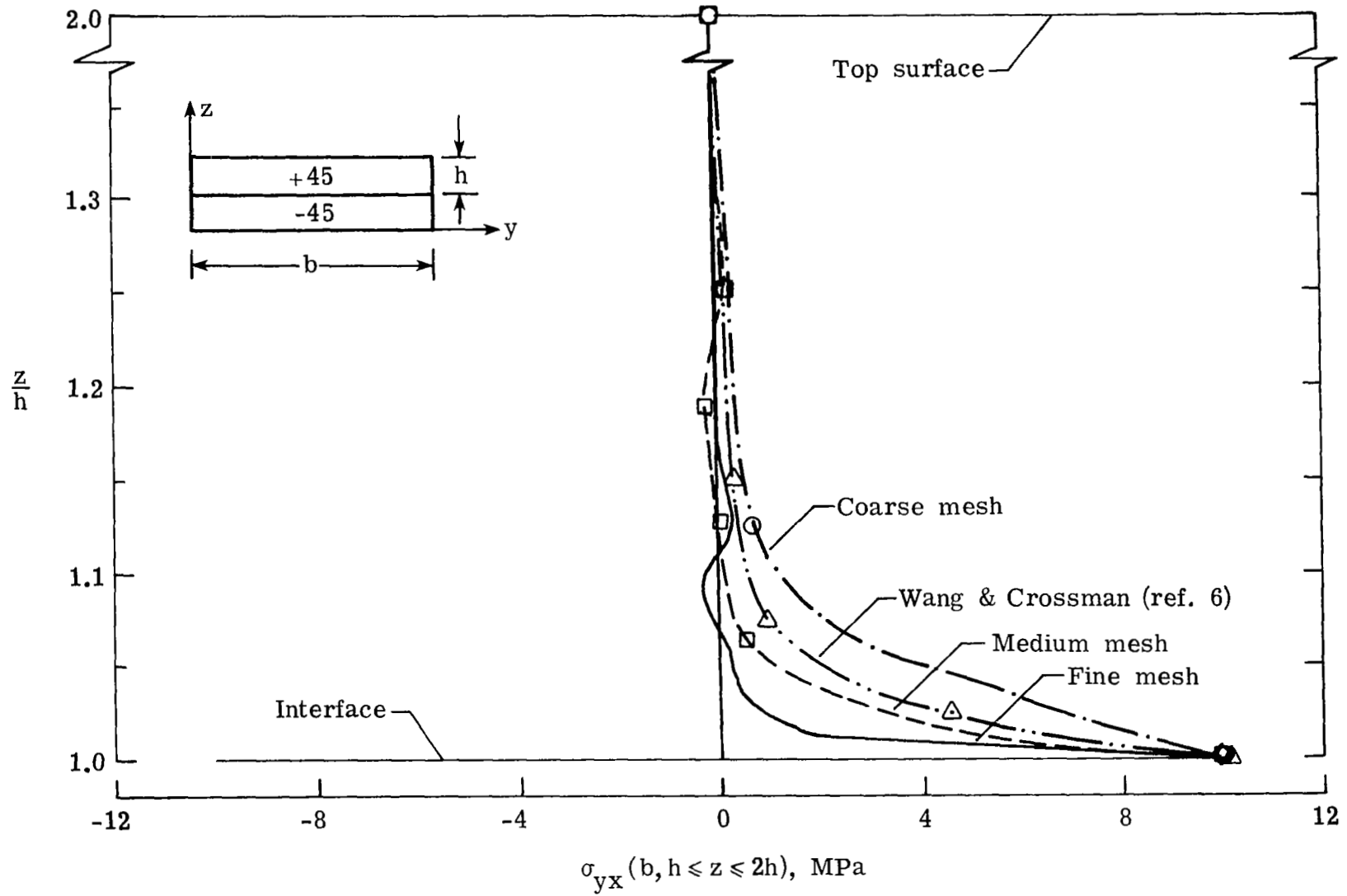


Figure 14.- Distribution of σ_{yx} through the thickness at the free edge in the +45 ply.

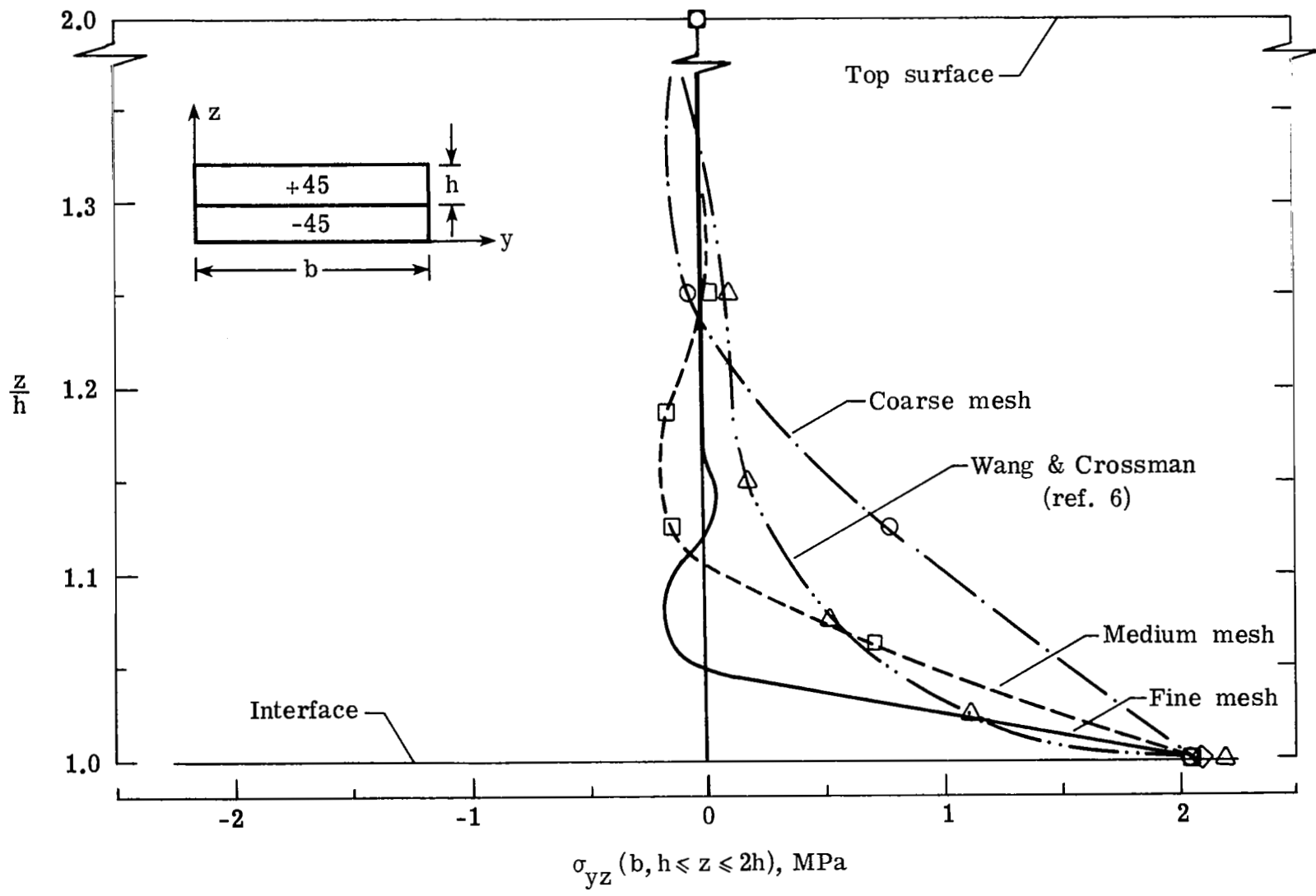
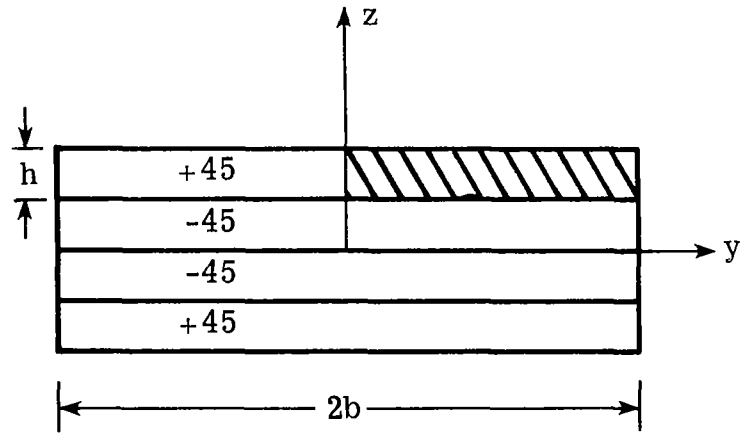
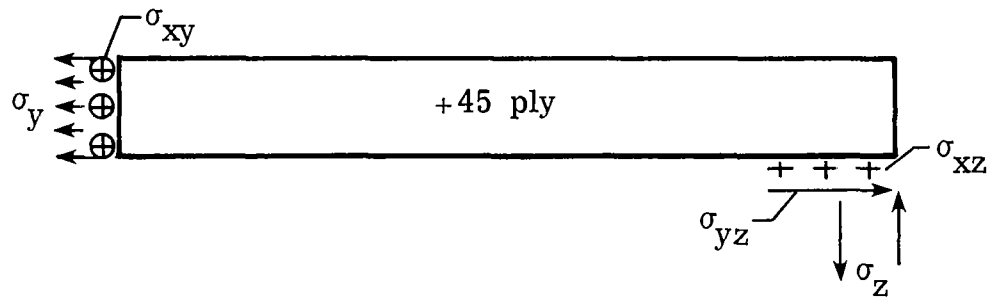


Figure 15.- Distribution of σ_{yz} through the thickness at the free edge in the +45 ply.

(a) $[\pm 45]_s$ laminate.

(b) Free body diagram of the top ply.

Figure 16.- Equilibrium conditions.

1. Report No. NASA TP-1751		2. Government Accession No.		3. Recipient's Catalog No.	
4. Title and Subtitle A NEW LOOK AT NUMERICAL ANALYSES OF FREE-EDGE STRESSES IN COMPOSITE LAMINATES				5. Report Date December 1980	
				6. Performing Organization Code 506-53-53-01	
7. Author(s) I. S. Raju, J. D. Whitcomb, and J. G. Goree				8. Performing Organization Report No. L-13777	
				10. Work Unit No.	
9. Performing Organization Name and Address NASA Langley Research Center Hampton, VA 23665				11. Contract or Grant No.	
				13. Type of Report and Period Covered Technical Paper	
12. Sponsoring Agency Name and Address National Aeronautics and Space Administration Washington, DC 20546				14. Sponsoring Agency Code	
15. Supplementary Notes I. S. Raju: The George Washington University, Joint Institute for Advancement of Flight Sciences, Langley Research Center, Hampton, Virginia. J. D. Whitcomb: Langley Research Center, Hampton, Virginia. J. G. Goree: Clemson University, Clemson, South Carolina.					
16. Abstract <p>The edge-stress problem for a $[\pm 45]_S$ graphite/epoxy laminate was examined in detail. A review of the literature of this problem showed that the interlaminar normal stress, σ_z, distributions along the interface between the $+45^\circ$ and -45° plies, obtained by various investigators, disagreed in magnitude and sign. Since a stress singularity exists at the intersection of the interface and the free edge, the differences in magnitude of the peak stress were expected, but not the difference in the sign. This paper investigates the reliability of the displacement-formulated finite element method in analyzing the edge-stress problem. Analyses of two well-known elasticity problems, one involving a stress discontinuity and one a singularity, showed that the finite element analysis yields accurate stress distributions everywhere except in two elements closest to the stress discontinuity or singularity. Stress distributions for a $[\pm 45]_S$ laminate showed the same behavior near the singularity found in the well-known problems with exact solutions. The displacement-formulated finite element method, therefore, appears to be a highly accurate technique for calculating interlaminar stresses in composite laminates. The disagreement among the numerical methods was attributed to the unsymmetric stress tensor at the singularity.</p>					
17. Key Words (Suggested by Author(s)) Composite laminates Stress singularity Interlaminar stresses Finite elements Stress discontinuity			18. Distribution Statement Unclassified - Unlimited Subject Category 39		
19. Security Classif. (of this report) Unclassified		20. Security Classif. (of this page) Unclassified		21. No. of Pages 34	22. Price A03